In situ Synthesis of a Mesoporous MIL-100(Fe) Bacteria Exoskeleton

Anastasia Permyakova,[†,‡] Alshaba Kakar,[†] Jonathan Bachir,[†] Effrosyni Gkaniatsou,[†] Bernard Haye,[‡] Nicolas Menguy,[§] Farid Nouar,[±] Christian Serre,[±] Nathalie Steunou,[†] Thibaud Coradin,[‡] Francisco M Fernandes[‡]* and Clémence Sicard[†]*

[†] *Institut Lavoisier de Versailles, UMR CNRS 8180, UVSQ, Université Paris-Saclay, 78035 Versailles, France*

[‡] *Laboratoire de Chimie de la Matière Condensée de Paris, UMR 7574, Sorbonne Université, F-75005, Paris, France*

[§] *Sorbonne Université, Muséum National d'Histoire Naturelle, UMR CNRS 7590, IRD. Institut de Minéralogie, de Physique des Matériaux et de Cosmochimie(IMPMC), Paris, France.*

[±] *Institut des Matériaux Poreux de Paris (IMAP), Ecole Normale Supérieure de Paris, ESPCI Paris, CNRS, PSL University, 75005 Paris, France.*

For correspondence:

*Francisco M Fernandes - E-mail: francisco.fernandes@sorbonne-université.fr

*Clémence Sicard - E-mail: clemence.sicard@uvsq.fr

Abstract

The mesoporous iron polycarboxylate MIL-100(Fe) was synthesized in presence of *Pseudomonas putida* bacteria. The synthesis was performed under green conditions, i.e. pure aqueous media at 30°C that were compatible with the preservation of the cell membrane integrity. Interestingly, the resulting bio-hybrid exhibited a very different microstructure than a physical mixture of the two components, as it led to the formation of a novel living material featuring an exoskeleton encapsulating individual bacteria cell. Interestingly, TEM and STEM on cross-sections revealed that this shell was not directly in contact with the cell wall, suggesting the exo-polysaccharides network promotes strong interactions with the MOF precursors leading to high proximity between the two components.

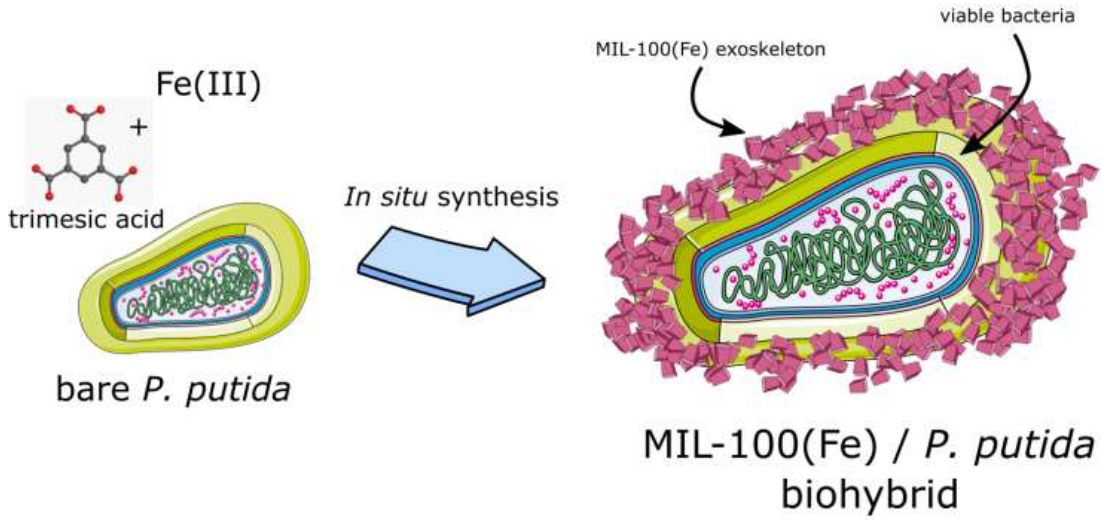

Living materials possess unique functionalities as they harness the specific capabilities of living organisms and the robustness and chemical versatility of organic, inorganic or hybrid materials. As a result, these are expected to play a highly significant role in applications as diverse as bioremediation, biocatalysis, probiotics, cell therapy, tissue engineering, and sensing.[1] Such bio-hybrid entities can be obtained either by cell colonization of a pre-formed scaffold or by *in situ* cell encapsulation depending on the material porosity, the reaction/process cytocompatibility and the targeted application.[2] One of the key challenges is to control the cells' local environment to ensure adequate physiological conditions required to preserve viability and biological activity. Microorganisms, such as bacteria or yeasts, usually require individual encapsulation —where each cell is coated by a material layer. Such exoskeleton can act as a physical barrier able to modulate the interactions with the external environment, reinforcing the resistance to external stressors (physicochemical, enzymatic, thermal, etc.) without hampering the molecular exchanges required to maintain the cellular homeostasis(nutrients, waste, etc..).[3] The ability to modulate the materials porosity is thus critical to design functional living materials. In this context Metal-Organic Frameworks (MOFs) provide unique platforms to design materials with *ad hoc* ordered porosity.

MOFs are porous hybrid crystalline solids, with tuneable chemical composition and structural features.[4] They have been successfully combined with proteins, allowing for their stabilization during storage or in denaturing conditions,[5–9] at the exception of some acidic Zr-MOFs that are associated with proteomic properties.[10] These promising results were extended to other biological entities,[11] including cells (yeasts,[12] mammalian cells,[13] red blood cells,[14] ...). However, this field is still in its infancy and, to date, only a few works concern MOF association with bacteria—whose relevance in the living materials domain is paramount.[15–20] The mismatch between bacteria size (in the micrometer range) and MOF pores (below 5 nm) excludes direct bacterial colonization within the MOFs internal porosity. Two alternative encapsulation strategies have thus been employed, either by assembly of preformed 2D-MOF sheets[20] or by the *in-situ* synthesis of MOF in presence of bacteria.[15–19] The main challenges lie in obtaining an intimately-assembled bio-hybrid while preserving bacteria integrity. The former strategy involves strong host-guest interactions between the MOF layer and the cell surface, which should be fine-tuned for each cell/MOF couple. The *in-situ* synthesis imposes a narrow window of synthetic conditions that is compatible with the cells' physiological requirements (i.e. water, mild temperatures, pH and low toxicity of MOF precursors). Few

MOFs can be obtained in such stringent conditions and, so far, only microporous Zinc Zeolitic Imidazolate Frameworks (ZIF), and mainly the hydrophobic ZIF-8, was assembled in presence of microorganisms.[15–18]

Here we widen the range of MOFs capable of encapsulating living cells by carrying out an *in-situ* synthesis of the iron polycarboxylate MIL-100(Fe) (MIL = Matériaux Institut Lavoisier). This MOF displays significantly different properties from the previously studied ZIFs (mesoporosity, hydrophilicity, chemical stability in water and low toxicity of the precursors)[21–23] and is thus complementary in terms of the functions brought to the biohybrid material. Since the physico-chemical properties of the MOFs (hydrophobicity or acidity) are indeed known to impact their affinity with biomolecules,[24,25] their rational modulation could provide an invaluable tool to design a whole novel class of materials, characterized by the specificity of biological entities and the chemical versatility of MOFs.

Pseudomonas putida CFBP 5039 was selected as a non-pathogen gram negative model bacterial strain of interest in bioremediation processes. The stationary phase of *P. putida* was selected (24 h growth with approximately $1.2 \pm 0.6.10^8$ CFU.mL^{-1}, **Figure. S1**) as the most adequate physiological state to prepare bio-hybrid materials since it yielded reproducible bacterial concentration, favouring a fine control over the synthetic conditions and is generally associated with an enhanced resistance of bacteria to external stresses.[26]

Identification of the experimental conditions allowing for both preservation of bacteria integrity and MOF formation requires a careful optimisation of the physico-chemical parameters. The synthesis of MIL-100(Fe) has recently been performed in ambient pressure and moderate temperature (below 60 °C) in aqueous solution[27]—conditions necessary to preserve the viability of *P. putida.* However, the toxicity of the precursors' solutions required further investigation to determine the best parameters (concentration of MOF precursors, incubation time, …) to limit cellular damage during synthesis. Bacteria were incubated with various concentrations of each precursor (iron nitrate and trimesic acid), up to the concentrations compatible with the synthesis of MIL-100(Fe) (26 mmol.L^{-1} and 17 mmol.L^{-1} of iron(III) nitrate and trimesic acid, respectively).[27]

Bacteria integrity was evaluated by means of a live/dead assay using propidium iodide (PI, a fluorescent probe that only permeates damaged cell membranes) and SYTO9 (a fluorescent probe that permeates healthy membranes) **(Figure S2 and S3)**. After 24 h incubation, the highest concentration of iron(III) nitrate (26 $mmol.l^{-1}$) was found to disrupt the cell membranes. Shorter incubation time (3 h) still revealed deleterious at such iron concentration since only a small fraction of the imaged bacteria displayed intact membranes. When the metal precursor was diluted twice, a larger proportion of undamaged bacteria could be observed after 3 h incubation and some even remained unaltered after 24 h. Similarly, diluted concentrations of trimesic acid were found to be more favourable for the viability of the strain.

Based on these observations, MIL-100(Fe) was synthesized under diluted conditions, with concentrations of iron(III) nitrate and trimesic acid of 13 $mmol.L^{-1}$ and 8.5 $mmol.L^{-1}$, respectively. The possibility to form MIL-100(Fe) using such conditions in aqueous media under mild temperature (30 °C) was first assessed without any bacterium. After 21 h of reaction, a solid phase was recovered and characterized by Powder X-Ray Diffraction (**Figure 1**), showing a crystalline structure with Bragg peaks in agreement with the calculated pattern of MIL-100(Fe). To prepare the biohybrid, the same synthesis was conducted in presence of *P. putida* (*ca* 4.10^7 $CFU.mL^{-1}$). The PXRD pattern of the resulting bio-hybrid material was fully consistent with that of MIL-100(Fe), indicating the successful *in-situ* synthesis of MIL-100(Fe) in the presence of the bacteria.

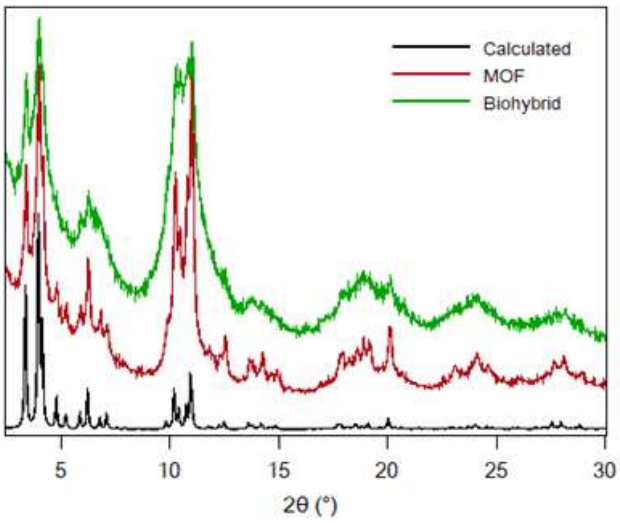

Figure 1. Powder X-Ray diffractions patterns (CuKα radiation, λ = 1.5418 Å) of MIL-100(Fe) calculated (black), synthesized without bacterium (red) and with bacteria (green).

The impact of MOF synthesis on the cellular integrity was further evaluated by live/dead assays as shown in **Figure 2(a-c)**. In the bio-hybrid, only few bacteria were stained by PI, suggesting that these conditions were compatible with the integrity of a large portion of the bacterial population.

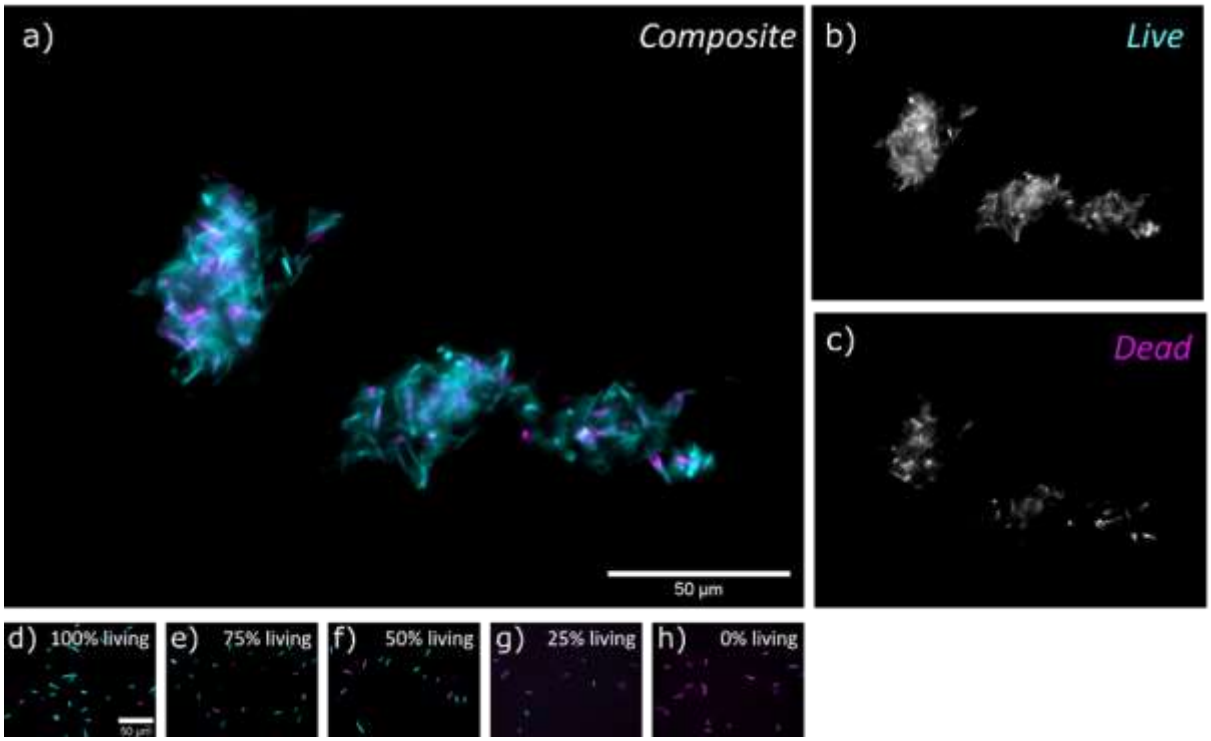

Figure 2. (a-c) Live/dead assay on the bio-hybrid. (a) Epifluorescence composite image of the bio-hybrid. Magenta codes for bacteria with damaged membranes permeated by PI and cyan codes for bacteria with intact cell membrane permeated by SYTO9. (b,c) Individual channels for live and dead bacteria, respectively. (d-h) Live/dead calibration image sequence from 100% live bacteria (d) to 0% live bacteria (h).

The microstructure of the bio-hybrid material was thoroughly examined to assess the interactions between MOF particles and bacteria. The spatial distribution of the two components in the bio-hybrid material was first evaluated by Scanning Electron Microscopy (**Figure 3**).The bare bacteria exhibited smooth surfaces whereas bacteria in the bio-hybrid material exhibited an irregular and rough topography, indicative of a granular shell covering the bacteria. This granular aspect was not observed for the control experiment when *P. putida* were mixed with pre-synthetized MIL-100(Fe) nanoparticles. Such experimental observations are in line with the formation of a cellular exoskeleton around *P. putida*, able to separate individual bacterial cells from their surroundings.

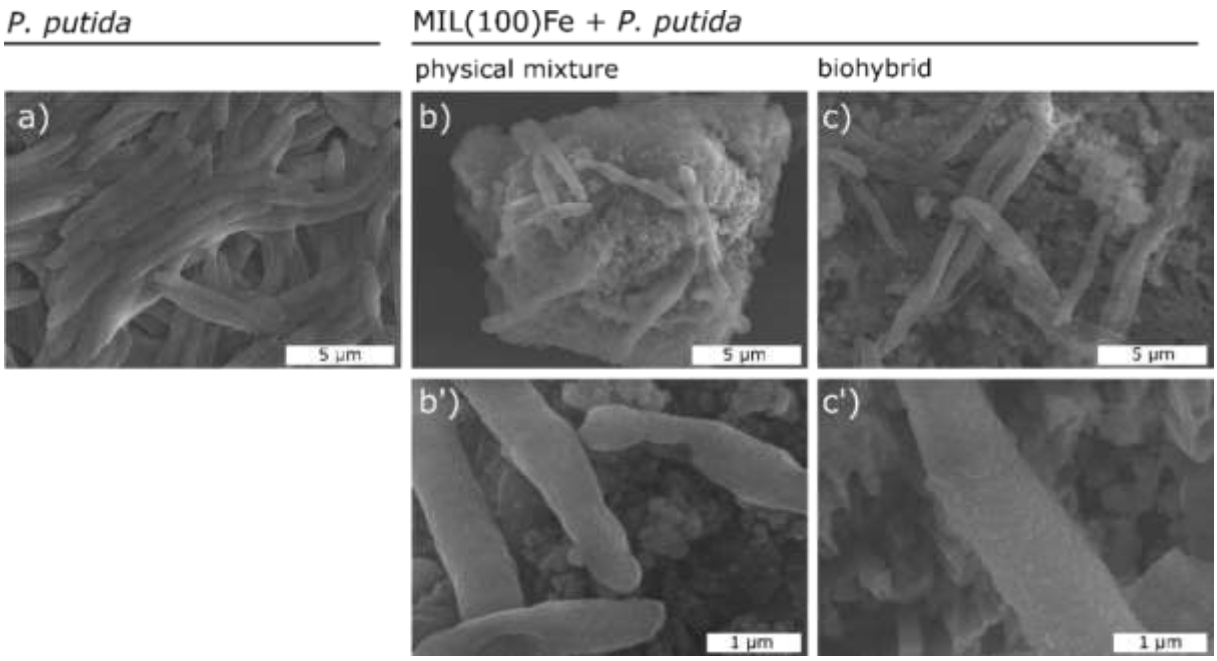

Figure 3. SEM images of a) bare *P. putida;* b, b') physical mixture between *P. putida* and MIL-100(Fe) and c, c') bio-hybrid.

To deepen our understanding of this intimate assembly, sample cross-sections obtained by ultramicrotomy were examined by Transmission Electron Microscopy (TEM) and scanning TEM using the high-angle annular dark-field mode (STEM-HAADF). Fixation and embedding protocols were optimized (**details in Supplementary Information**) to prevent sample degradation. As shown in **Figure 4**, TEM and STEM-HAADF images revealed that the bacteria membranes were preserved, in full agreement with the live/dead assays discussed above.These observations also underlined the presence of a 30 to 60 nm thick shell surrounding single bacterium (**Figure 4**), visible on most of the imaged bacteria (**Figure S4**).

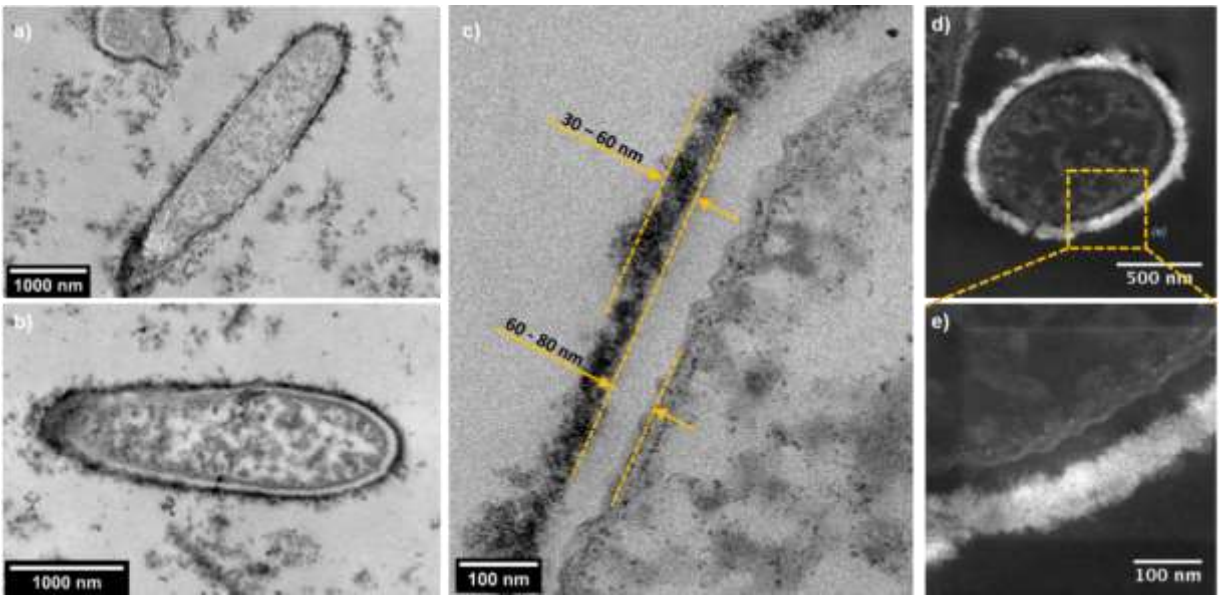

Figure 4. TEM images (a,b,c) and STEM-HAADF images (d,e) of bio-hybrid material cross-sections.

The chemical composition of the shell was probed by STEM-XEDS (**Figure 5**), indicating the presence of Fe elements, not detected with bare *P. Putida* (**Figure S5**). Note that electron diffraction could not be performed to confirm the crystalline nature of the shell, as the high carbon content of the sample prevents experiments at high voltage or sufficient acquisition time before degradation of the sample.Fe elements were also detected inside a few cells (**Figure S6**), in agreement with the iron uptake ability of *P. Putida*.[28] Interestingly, such an uptake did not prevent the formation of the particulate shell around the cell.

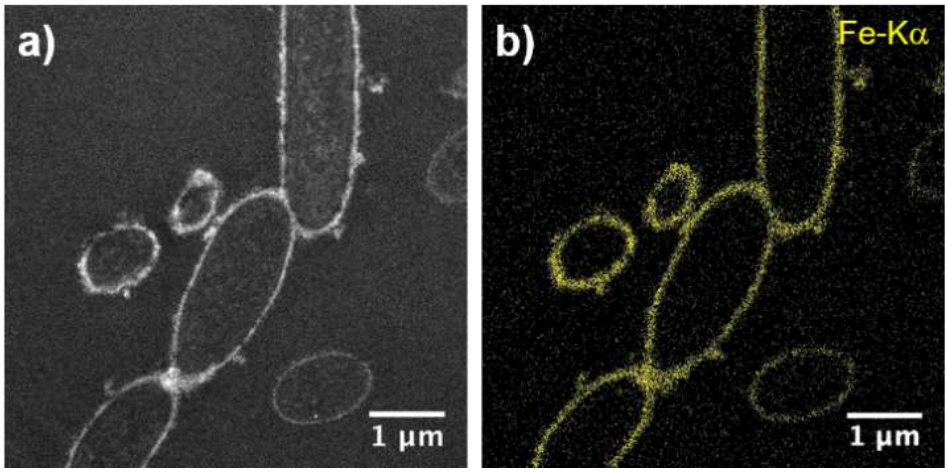

Figure 5. (a) STEM-HAADF image and (b) STEM-XEDS elemental mapping of the bio-hybrid material.

Remarkably, the MOF nanoparticles were not found directly attached to the cell wall but at a distance of *ca* 60-80 nm (**Figure 4**). This may be explained by the presence of an exopolysaccharide (EPS) network surrounding the bacterium. Many gram-negative bacteria strains,[29] including *P. putida*,[30] secrete EPS into their surrounding environment during their growth, especially during their stationary phase.We thus hypothesized that the functional groups (hydroxyl, carboxyl, amino...) of the EPS network may locally interact with Fe ions and act as a template for MIL-100(Fe) particles formation by generating a high density of heterogeneous nucleation sites at the cell surrounding. This is in agreement with previous works where carbohydrates were shown to induce ZIF-8 crystallization thanks to interactions between carbohydrates functional groups and Zn^{2+} ions.[31,32]

During this study, no evidence could however be found that MIL-100(Fe) formation was specifically triggered by the presence of bacteria. However, their EPS seemed to promote sufficient interactions with the MOF precursors, leading to the formation of an exoskeleton. This assumption was further supported by SEM and TEM images of bare MIL-100(Fe) particles prepared in absence of bacteria (**Figure S7**). These particles displayed a different size and morphology from those constituting the exoskeleton, reinforcing the putative role of the surface of the bacteria during the *in-situ* formation of MOF. Further understanding of the mechanisms at play is currently under investigation.

In conclusion, the mesoporous iron polycarboxylate, MIL-100(Fe), was synthetized in aqueous media at 30 °C in presence of bacteria with preservation of cellular membrane integrity. This work expands the structure and chemical compositions of MOFs that can be directly synthesized in presence of biological entities by addressing successfully the direct growth of a benchmark biocompatible iron MOFs coating living bacteria. While preservation of membrane integrity offers a strong indication of the cytocompatibility of the process, the metabolic functions of encapsulated cells are currently being investigated and will be reported in a near future. These results provide exciting new leads into novel MOF-based living materials with unique properties for applications in biotechnology and biomedical science.

Acknowledgements

The authors thank Dr. C. Livage and I. Génois for SEM experiments.

Funding Sources

This work was supported by the Paris Ile-de France Region - DIM Respore and the French National Research Agency (ANR) through the EMERGE project, grant n° ANR-18-CE08-0023-01 and the CellsInFoams project, grant n° ANR-17-CE08-0009.

References

(1) Rodrigo-Navarro, A.; Sankaran, S.; Dalby, M. J.; del Campo, A.; Salmeron-Sanchez, M. Engineered Living Biomaterials. *Nat. Rev. Mater.* **2021**, *6* (12), 1175–1190. https://doi.org/10.1038/s41578-021-00350-8.

(2) Parisi, C.; Qin, K.; Fernandes, F. M. Colonization versus Encapsulation in Cell-Laden Materials Design: Porosity and Process Biocompatibility Determine Cellularization Pathways. *Philos. Trans. R. Soc. A Math. Phys. Eng. Sci.* **2021**, *379* (2206), 20200344. https://doi.org/10.1098/rsta.2020.0344.

(3) Park, J. H.; Yang, S. H.; Lee, J.; Ko, E. H.; Hong, D.; Choi, I. S. Nanocoating of Single Cells: From Maintenance of Cell Viability to Manipulation of Cellular Activities. *Adv. Mater.* **2014**, *26* (13), 2001–2010. https://doi.org/10.1002/adma.201304568.

(4) Jiang, H.; Alezi, D.; Eddaoudi, M. A Reticular Chemistry Guide for the Design of Periodic Solids. *Nat. Rev. Mater.* **2021**, *6* (6), 466–487. https://doi.org/10.1038/s41578-021-00287-y.

(5) Liang, W.; Wied, P.; Carraro, F.; Sumby, C. J.; Nidetzky, B.; Tsung, C.; Falcaro, P.; Doonan, C. J. Metal–Organic Framework-Based Enzyme Biocomposites. *Chem. Rev.* **2021**, *121* (3), 1077–1129. https://doi.org/10.1021/acs.chemrev.0c01029.

(6) Huang, S.; Kou, X.; Shen, J.; Chen, G.; Ouyang, G. "Armor-Plating" Enzymes with Metal–Organic Frameworks (MOFs). *Angew. Chemie Int. Ed.* **2020**, *59* (23), 8786–8798. https://doi.org/10.1002/anie.201916474.

(7) Drout, R. J.; Robison, L.; Farha, O. K. Catalytic Applications of Enzymes Encapsulated in Metal–Organic Frameworks. *Coord. Chem. Rev.* **2019**, *381*, 151–160. https://doi.org/https://doi.org/10.1016/j.ccr.2018.11.009.

(8) Gkaniatsou, E.; Sicard, C.; Ricoux, R.; Mahy, J.-P.; Steunou, N.; Serre, C. Metal–Organic Frameworks: A Novel Host Platform for Enzymatic Catalysis and Detection. *Mater. Horizons* **2017**, *4* (1), 55–63. https://doi.org/10.1039/C6MH00312E.

(9) Wang, X.; Lan, P. C.; Ma, S. Metal–Organic Frameworks for Enzyme Immobilization: Beyond Host Matrix Materials. *ACS Cent. Sci.* **2020**, *6* (9), 1497–1506. https://doi.org/10.1021/acscentsci.0c00687.

(10) Wang, S.; Ly, H. G. T.; Wahiduzzaman, M.; Simms, C.; Dovgaliuk, I.; Tissot, A.; Maurin, G.; Parac-Vogt, T. N.; Serre, C. A Zirconium Metal-Organic Framework with SOC Topological Net for Catalytic Peptide Bond Hydrolysis. *Nat. Commun.* **2022**, *13* (1), 1284. https://doi.org/10.1038/s41467-022-28886-5.

(11) Velásquez-Hernández, M. de J.; Linares-Moreau, M.; Astria, E.; Carraro, F.; Alyami, M. Z.; Khashab, N. M.; Sumby, C. J.; Doonan, C. J.; Falcaro, P. Towards Applications of Bioentities@MOFs in Biomedicine. *Coord. Chem. Rev.* **2021**, *429*, 213651. https://doi.org/10.1016/j.ccr.2020.213651.

(12) Liang, K.; Richardson, J. J.; Doonan, C. J.; Mulet, X.; Ju, Y.; Cui, J.; Caruso, F.; Falcaro, P. An Enzyme-Coated Metal-Organic Framework Shell for Synthetically Adaptive Cell Survival. *Angew. Chemie Int. Ed.* **2017**, *56* (29), 8510–8515. https://doi.org/10.1002/anie.201704120.

(13) Zhu, W.; Guo, J.; Amini, S.; Ju, Y.; Agola, J. O.; Zimpel, A.; Shang, J.; Noureddine, A.; Caruso, F.; Wuttke, S.; Croissant, J. G.; Brinker, C. J. SupraCells: Living Mammalian Cells Protected within Functional Modular Nanoparticle-Based Exoskeletons. *Adv. Mater.* **2019**, *31* (25), 1900545. https://doi.org/10.1002/adma.201900545.

(14) Zhu, W.; Guo, J.; Agola, J. O.; Croissant, J. G.; Wang, Z.; Shang, J.; Coker, E.; Motevalli, B.; Zimpel, A.; Wuttke, S.; Brinker, C. J. Metal–Organic Framework Nanoparticle-Assisted Cryopreservation of Red Blood Cells. *J. Am. Chem. Soc.* **2019**, *141* (19), 7789–7796. https://doi.org/10.1021/jacs.9b00992.

(15) Luzuriaga, M. A.; Herbert, F. C.; Brohlin, O. R.; Gadhvi, J.; Howlett, T.; Shahrivarkevishahi, A.; Wijesundara, Y. H.; Venkitapathi, S.; Veera, K.; Ehrman, R.; Benjamin, C. E.; Popal, S.; Burton, M. D.; Ingersoll, M. A.; De Nisco, N. J.; Gassensmith, J. J. Metal–Organic Framework Encapsulated Whole-Cell Vaccines Enhance Humoral Immunity against Bacterial Infection. *ACS Nano* **2021**, *15* (11), 17426–17438. https://doi.org/10.1021/acsnano.1c03092.

(16) Wei, H.; Yang, X.-Y.; Geng, W.; van der Mei, H. C.; Busscher, H. J. Interfacial Interactions between Protective, Surface-Engineered Shells and Encapsulated Bacteria with Different Cell Surface Composition. *Nanoscale* **2021**, *13* (15), 7220–7233.

https://doi.org/10.1039/D0NR09204E.

(17) Chen, W.; Kong, S.; Lu, M.; Chen, F.; Cai, W.; Du, L.; Wang, J.; Wu, C. Comparison of Different Zinc Precursors for the Construction of Zeolitic Imidazolate Framework-8 Artificial Shells on Living Cells. *Soft Matter* **2020**, *16* (1), 270–275. https://doi.org/10.1039/C9SM01907C.

(18) Liang, K.; Richardson, J. J.; Cui, J.; Caruso, F.; Doonan, C. J.; Falcaro, P. Metal-Organic Framework Coatings as Cytoprotective Exoskeletons for Living Cells. *Adv. Mater.* **2016**, *28* (36), 7910–7914. https://doi.org/10.1002/adma.201602335.

(19) Li, H.; Kang, A.; An, B.; Chou, L.-Y.; Shieh, F.-K.; Tsung, C.-K.; Zhong, C. Encapsulation of Bacterial Cells in Cytoprotective ZIF-90 Crystals as Living Composites. *Mater. Today Bio* **2021**, *10* (February), 100097. https://doi.org/10.1016/j.mtbio.2021.100097.

(20) Ji, Z.; Zhang, H.; Liu, H.; Yaghi, O. M.; Yang, P. Cytoprotective Metal-Organic Frameworks for Anaerobic Bacteria. *Proc. Natl. Acad. Sci.* **2018**, *115* (42), 10582–10587. https://doi.org/10.1073/pnas.1808829115.

(21) Horcajada, P.; Surblé, S.; Serre, C.; Hong, D.-Y.; Seo, Y.-K.; Chang, J.-S.; Grenèche, J.-M.; Margiolaki, I.; Férey, G. Synthesis and Catalytic Properties of MIL-100(Fe), an Iron(III) Carboxylate with Large Pores. *Chem. Commun.* **2007**, *100* (27), 2820–2822. https://doi.org/10.1039/B704325B.

(22) Christodoulou, I.; Bourguignon, T.; Li, X.; Patriarche, G.; Serre, C.; Marlière, C.; Gref, R. Degradation Mechanism of Porous Metal-Organic Frameworks by In Situ Atomic Force Microscopy. *Nanomaterials* **2021**, *11* (3), 722. https://doi.org/10.3390/nano11030722.

(23) Sene, S.; Marcos-Almaraz, M. T.; Menguy, N.; Scola, J.; Volatron, J.; Rouland, R.; Grenèche, J. M.; Miraux, S.; Menet, C.; Guillou, N.; Gazeau, F.; Serre, C.; Horcajada, P.; Steunou, N. Maghemite-NanoMIL-100(Fe) Bimodal Nanovector as a Platform for Image-Guided Therapy. *Chem* **2017**, *3* (2), 303–322. https://doi.org/10.1016/j.chempr.2017.06.007.

(24) Liang, W.; Xu, H.; Carraro, F.; Maddigan, N. K.; Li, Q.; Bell, S. G.; Huang, D. M.; Tarzia, A.; Solomon, M. B.; Amenitsch, H.; Vaccari, L.; Sumby, C. J.; Falcaro, P.; Doonan, C. J. Enhanced Activity of Enzymes Encapsulated in Hydrophilic Metal–Organic Frameworks. *J. Am. Chem. Soc.* **2019**, *141* (6), 2348–2355. https://doi.org/10.1021/jacs.8b10302.

(25) Gkaniatsou, E.; Ricoux, R.; Kariyawasam, K.; Stenger, I.; Fan, B.; Ayoub, N.; Salas, S.; Patriarche, G.; Serre, C.; Mahy, J.-P.; Steunou, N.; Sicard, C. Encapsulation of Microperoxidase-8 in MIL-101(Cr)-X Nanoparticles: Influence of Metal–Organic Framework Functionalization on Enzymatic Immobilization and Catalytic Activity. *ACS Appl. Nano Mater.* **2020**, *3* (4), 3233–3243. https://doi.org/10.1021/acsanm.9b02464.

(26) Corcoran, B. M.; Ross, R. P.; Fitzgerald, G. F.; Stanton, C. Comparative Survival of Probiotic Lactobacilli Spray-Dried in the Presence of Prebiotic Substances. *J. Appl. Microbiol.* **2004**, *96* (5), 1024–1039. https://doi.org/10.1111/j.1365-2672.2004.02219.x.

(27) Panchal, M.; Nouar, F.; Serre, C.; Benzaqui, M.; Sene, S.; Steunou, Nathalie Giménez-Marques, M. EP3357929A1 Low Temperature Process for the Synthesis of MOF Carboxylate Nanoparticles, 2017.

(28) Molina, L.; Geoffroy, V. A.; Segura, A.; Udaondo, Z.; Ramos, J.-L. Iron Uptake Analysis in a Set of Clinical Isolates of Pseudomonas Putida. *Front. Microbiol.* **2016**, *7* (December), 496. https://doi.org/10.3389/fmicb.2016.02100.

(29) Sutherland, I. W. Microbial Polysaccharides from Gram-Negative Bacteria. *Int. Dairy J.* **2001**, *11*, 663–674. https://doi.org/10.1016/S0958-6946(01)00112-1

(30) Celik, G. Y.; Aslim, B.; Beyatli, Y. Characterization and Production of the Exopolysaccharide (EPS) from Pseudomonas Aeruginosa G1 and Pseudomonas Putida G12 Strains. *Carbohydr. Polym.* **2008**, *73* (1), 178–182. https://doi.org/10.1016/j.carbpol.2007.11.021.

(31) Astria, E.; Thonhofer, M.; Ricco, R.; Liang, W.; Chemelli, A.; Tarzia, A.; Alt, K.; Hagemeyer, C. E.; Rattenberger, J.; Schroettner, H.; Wrodnigg, T.; Amenitsch, H.; Huang, D. M.; Doonan, C. J.; Falcaro, P. Carbohydrates@MOFs. *Mater. Horizons* **2019**, *6* (5), 969–977. https://doi.org/10.1039/C8MH01611A.

(32) Liang, K.; Wang, R.; Boutter, M.; Doherty, C. M.; Mulet, X.; Richardson, J. J. Biomimetic Mineralization of Metal–Organic Frameworks around Polysaccharides. *Chem. Commun.* **2017**, *53* (7), 1249–1252. https://doi.org/10.1039/C6CC09680H.